BOLLETTINO DI GEOFISICA TEORICA ED APPLICATA VOL. XXXV, N. 139 - SEPTEMBER 1993

G. NERI[1] and M. WYSS[2]

# PRELIMINARY RESULTS FROM STRESS TENSOR INVERSION OF EARTHQUAKE FAULT-PLANE SOLUTIONS IN THE SOUTHERN TYRRHENIAN REGION

**Abstract.** The method of Gephart and Forsyth (1984) for stress tensor inversion from earthquake fault-plane solutions has been applied to 39 crustal seismic events from the region which includes Southern Calabria, Northeastern Sicily and the Aeolian Islands. We conclude that the stress tensor directions are not uniform in the study area because the misfit of the inversion is large if the entire data set is used, but the misfits for inversion of data from sub-regions are small. This result is expected on the basis of the geodynamic information available for the area. Inversion for the stress tensor in separate sub-volumes, defined according to the main structural features of the area, shows that the directions of the greatest principal stress vary from near vertical in Calabria to near horizontal with a strike of N20E in eastern Sicily. These "best models" agree with geologic and tectonic data. At present, the difference in stress directions between the sub-volumes studied can only be asserted at a confidence level between 50% and 75%, due to the low number of earthquakes suitable for the application of the inversion procedure in each sub-volume. For this reason, the stress space variation in the Southern Tyrrhenian region needs to be the subject of further investigations with richer data samples, but the present work is a useful basis for them, and for network improvements aimed at a development of this research topic.

## INTRODUCTION

During recent years, the increasing number of seismic stations in Sicily and Calabria has allowed a start to be made with several types of investigation on microearthquake activity, such as accurate hypocenter location (Neri et al., 1991), fault-plane solution computation and comparisons with geological information (Neri et al., 1993). In this context, a preliminary approach to stress tensor inversion from fault plane solutions (FPS) appears to be appropriate: it should provide a preliminary contribution to research into the geodynamical processes in the region, and will be useful for the better planning of future research effort and network operations.

Stress tensor inversion has been carried out in recent years in several areas (Gephart and Forsyth, 1984; Michael, 1984a, 1984b; Oppenheimer et al., 1988; Jones, 1988; Hauksson, 1990; Liang and Wyss, 1991; Gillard et al., 1992; Wyss et al., 1992a, 1992b). It has helped scientists in identifying, among other things, stress space-time patterns, relationships between stress variations and strong earthquakes, with the identification of fault planes and estimates of their relative weakness, and with modelling the strain accumulation mechanisms. Thus, this method is useful for tectonic modelling and source-process investigations.

Following these experiences, we intend to apply the method of Gephart and Forsyth (1984) to earthquakes that have occurred in the area which includes the Southern Tyrrhenian Sea and the Calabrian arc (Figs. 1 and 4) during the period 1988-1991. As will be described in the next paragraph, the area under investigation is located in the bulk of the contact belt between



Manuscript received February 5, 1993; accepted August 2, 1993.

[1] Istituto Geofisico e Geodetico, University of Messina, Italy.

[2] Geophysical Institute, University of Alaska, Fairbanks, USA.

the African and Euroasiatic plates, so that studying the tectonic stress distribution in it may contribute to solving the very complex puzzle of Mediterranean geodynamics.

Basically, the purpose of this paper is to test the hypothesis that all the different fault-plane solutions throughout the entire source volume investigated could be due to a single stress tensor orientation, with the differences in solutions being caused by the availability of different planes of weakness for faulting. For example, if a set of near vertical, and another set of near horizontal planes of weakness are available, a single orientation of the stress tensor can cause slip on both of these planes in separate earthquakes. In this case, a heterogeneous set of fault plane solutions may actually reflect a homogeneous stress field. Alternatively, it may be that the differences in fault-plane solutions define spatial differences in the stress tensor orientation in the area investigated, as may be expected in our specific case in the light of available information on the local geology and tectonics (next paragraph). Thus, we invert for the orientation of the stress tensor and compute the confidence limits for the data set and for subsets from different crustal volumes. The choice of crustal volumes is based on tectonic information other than the data analyzed. An a priori limitation of our investigation is represented by the number of available earthquakes. Their number is unfortunately not large enough to provide good constraints on the direction of the main stress axes, and limits the number of sub-volumes we may investigate. This relatively small number of fault-plane solutions is the reason for which this work is only preliminary.

## GEODYNAMIC CONTEXT

The southern Tyrrhenian lithosphere is characterized (see for example Morelli et al., 1975; Calcagnile and Panza, 1981; Calcagnile et al., 1982; Scarpa, 1982) by a quite uniform thickening both of crust and lid from the abyssal plain to the Calabrian arc (Figs. 1 and 3), associated with a decrease in the surface heat flow (Loddo and Mongelli, 1979) and gravity (Colombi et al., 1973; Morelli et al., 1975). Geological observations (see among others Frazzetta et al., 1982; Ghisetti and Vezzani, 1982) and DSS surveys (Finetti and Del Ben, 1986) reveal the presence of NW-SE to E-W transcurrent faults characterized by dextral mechanisms in the southern sector (Filicudi, Sisifo, Vulcano and Taormina faults, Fig. 1) and by sinistral ones to the north (Palinuro and Policastro faults, same figure). Along the Calabrian arc, there is a notable heterogeneity of mechanisms although graben-like structures parallel to the arc (Figs. 1 and 2) appear to be the most important from the seismological point of view, since they have been the sites of the most intense regional earthquakes over the last centuries (magnitude 6 to 7; Mulargia and Boschi, 1983; Martini and Scarpa, 1983; Bottari and Lo Giudice, 1987). The lithosphere beneath the Southern Tyrrhenian Sea is characterized by less energetic seismicity (maximum magnitude values in the range 5-6; Falsaperla et al., 1989). Also, a well known seismic feature of the Southern Tyrrhenian region is represented by the occurrence of deep earthquake activity (reaching a depth of about 500 km) along a Wadati-Benioff plane dipping to the northwest (see for example Gasparini et al., 1982; Anderson and Jackson, 1987).

Several tectonic models have been proposed in the last two decades for this region, and the debate is still open. Barberi et al. (1973) hypothesized the existence of an active subduction process, and interpreted the Southern Tyrrhenian area as a back-arc basin. Rifting processes were hypothesized in the papers by Scandone (1979), Scandone and Patacca (1984), Finetti and Del Ben (1986), Patacca and Scandone (1989), and Patacca et al. (1990). Locardi (1988) proposes a model which assumes the growth of diapiric structures throughout the Tyrrhenian region. According to Mantovani et al. (1985, 1987 and 1990), the dynamics of the Tyrrhenian region are controlled by the rotation of the Adriatic microplate around a pole located in the Alpine chain, in the framework of the compression exerted by the African plate. In any case, it is evident that the geodynamical situation in this region is complex. Several microplates, blocks and structural units, possibly deriving from the consumption and fracturing of the old margins of the African and Euroasiatic plates are present. This may produce a high degree of heterogeneity in the tectonic stress distribution. Among other things, an important feature of this region shared by the above models is the kinematics of the Southern Tyrrhenian lithosphere, which should be affected by movements towards the southeast (Figs. 2 and 3).

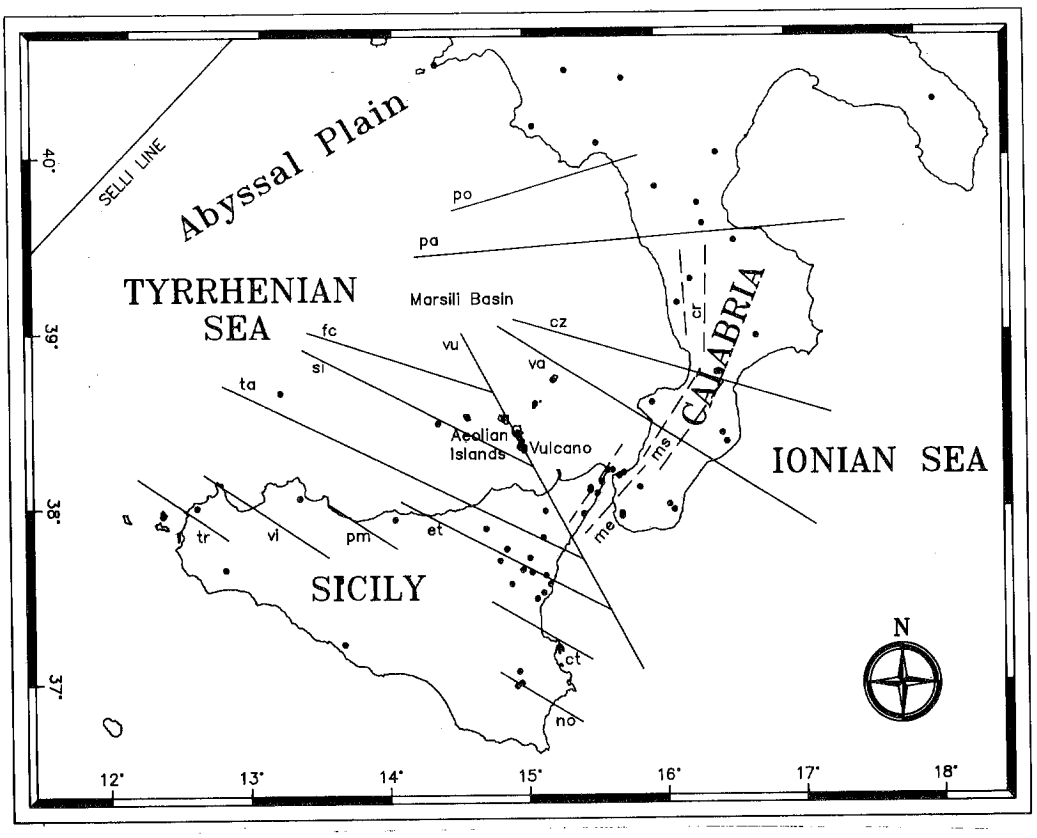


Fig. 1 - Map of the area under investigation, with locations of the seismic stations (circles) and of the main fault systems (pm = Palermo; ct = Catania; et = Etna; ta = Taormina; si = Sisifo; fc = Filicudi; vu = Vulcano; va = Capo Vaticano; cz = Catanzaro; pa = Palinuro; po = Policastro; me = Messina; ms = Mesima: cr = Crati). Geological information is mostly taken from Ghisetti and Vezzani (1982) and Finetti and Del Ben (1986).

The information given by Finetti and Del Ben (1986), and Patacca et al. (1990) appears to be the most suitable (in level of detail) for an evaluation of the results of the present seismological investigation. According to Finetti and Del Ben (1986), the kinematics of the Southern Tyrrhenian lithosphere are sustained by an opening process occurring along the Selli line (Figs. 1 and 2); the lithospheric mass migration towards the southeast has been characterized by a gradually decreasing intensity since the Middle-Upper Pliocene and, in most recent times, has mainly affected the most internal structures of the original front (between the Sisifo and Palinuro faults, Figs. 1 and 2). In the framework of the rifting process, Patacca et al. (1990) maintain that a notable episode of new crust generation probably started during the Lower Pleistocene in the Marsili basin (Fig. 1). As will be discussed later, such a space differentiation of the crustal generation process is in agreement with the space variation of the stress tensor that we have found in this study.

The deep earthquake activity is explained by several authors (Scandone, 1979; Gasparini et al., 1982; Finetti and Del Ben, 1986; Patacca et al., 1990) in terms of passive subduction of a lithospheric slab which was active before the Tyrrhenian opening and has suffered high stretching and distortion by the above mentioned movements of the lithosphere towards the southeast (Fig. 3). In the model of Patacca and Scandone (1989), and Patacca et al. (1990), the sinking of the slab is fundamental to the development of the opening process, as well as to the mountain building in the Appeninic chain, and the tensional stresses observed along the same chain (Fig. 2). More precisely, geological investigations carried out by Burton (1964) and Ghisetti (1980) showed that the Peloritani and Aspromonte chains (Figs. 2 and 3) have

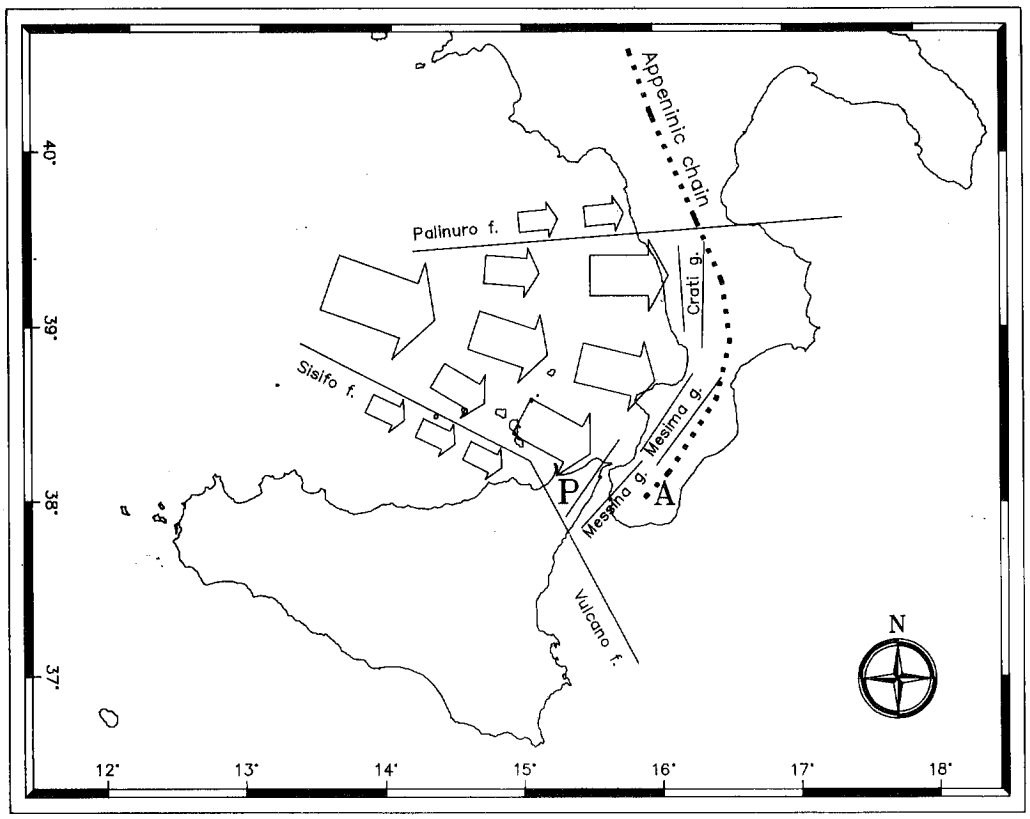


Fig. 2 - Schematic planimetric representation of kinematic processes in the Southern Tyrrhenian lithosphere. The lithospheric mass between the Palinuro and Sisifo-Vulcano faults migrates with a greater speed than that to the north and the south. The main graben structures of the Calabrian Arc (Crati, Mesima and Messina) are also shown. Letters P and A indicate the locations of the Peloritani and Aspromonte ranges.

been uplifting in recent geological times at a rate of about 1 mm/yr. According to Mulargia et al. (1984), this process has probably been taking place aseismically, and seems to be confirmed currently by the available tidal and levelling measurements. Tensional stresses are also present along the same chains (Figs. 2 and 3), as clearly testified by notable subsidences affecting the Messina Strait coastlines and other structures of the Calabrian arc during the most intense phases of local seismic activity (Martini and Scarpa, 1983; Mulargia et al., 1984; Bottari et al., 1989). However, only the upper crust seems to be affected by these tensional stresses, while below, thrusting of the Tyrrhenian crust on the Ionian is hypothesized in a ductile (and then aseismic) environment (Ghisetti, 1984; Fig. 3). In the light of this information, the normal structures may be considered dominant over the thrusts from the point of view of seismic effects.

It is possible to furnish a unified view of all these processes (Patacca et al., 1990; Neri et al., 1993; Fig. 3). In fact, the sinking of the old and nowadays passive subduction structure deepening to the NW beneath the Southern Tyrrhenian Sea would produce a relaxation of the Southern Tyrrhenian lithosphere and, consequently, (1) mass migration toward the Calabrian arc, (2) thrusting on the Ionian lithospheric structure, and (3) the propagation of a relaxation wave which is the basis of the Appenines mountain building. Reasonably, tensional stresses and graben structures appear on the top of this "uplift tranversal wave".

## DATA

Local earthquake data reported in the 1988-1991 bulletins of the networks operating in

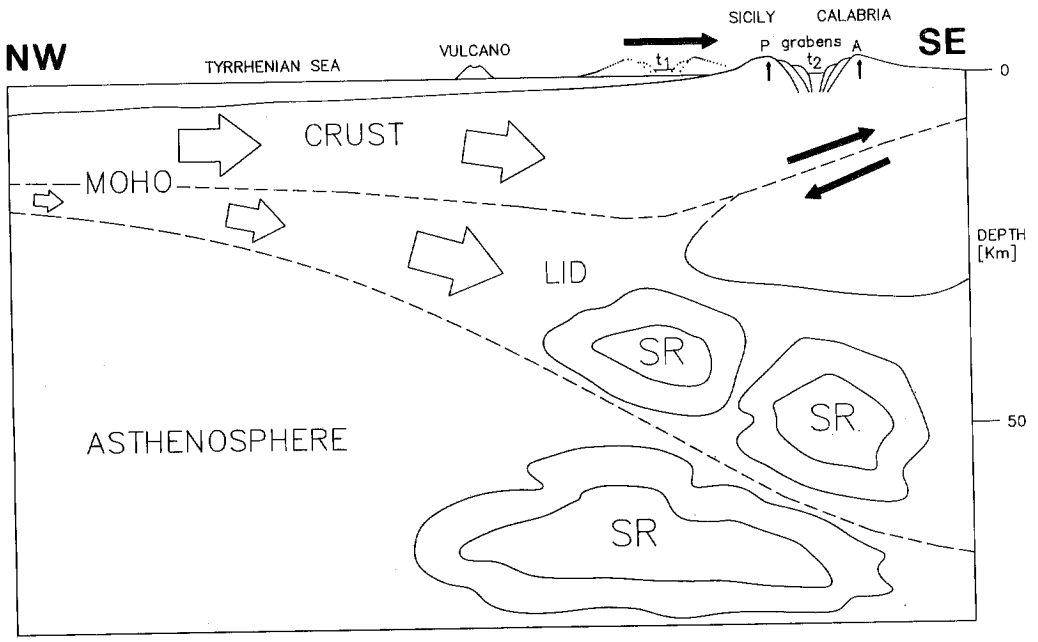


Fig. 3 - NW-SE vertical section through Vulcano with indication of kinematic processes (empty arrows) and slab remnants (SR). "t1" and "t2" indicate two different time instants ("t2" corresponds to the present); the horizontal full arrow close to them indicates the sense of propagation of the presumed relaxation wave which could be at the basis of the Peloritani (P) and Aspromonte (A) mountain building; tensional stresses and graben structures appear on the top of this "uplift transversal wave".

Sicily and Calabria (a station map is given in Fig. 1) were used in the investigation. Only events with epicenter in the sector 37.5-39N 14-16.5E, duration magnitude greater than 2.5, and at least 10 P-polarities were considered (73 events in total).

After having selected for each event the recording stations leading to the best network geometry possible with the available data, an improved hypocenter location of the earthquakes was computed using the HYPO71PC computer program (Lee and Valdes, 1989), and a 1-D velocity model with station corrections recently determined for the area (Neri et al., 1991). The results are given in Table 1. Twenty earthquakes showed D-quality locations and were eliminated from the sample. For the remaining 53, the fault-plane solutions were computed (Whitcomb et al., 1973). A quantitative evaluation of the FPS quality was not possible because the number of stations was not in general high enough to permit this. Therefore, we judged subjectively whether the solution was constrained well enough for the application of the stress tensor inversion procedure. In particular, if one of the fault-planes was unconfined to 40°, the solution was excluded. By following this criterion, 35 events were selected. They can be identified in Table 1 where their location area is indicated (Sis=Sisifo fault; Vul=Vulcano fault; Dep=subcrustal events; Cal=Calabrian arc; Out=other events; see also Fig. 4). Some additional information concerning the data set used for computing the FPS of each event is also given in the same table by reporting the variable "Pol", which represents the ratio between the number of polarities in agreement with the fault plane solution and the total number of polarities. This earthquake sample has been augmented by four fault-plane solutions from the literature (see caption of Fig. 4 for details). Epicenters and FPS for the whole sample (39 events) are shown in Figs. 4 and 5, respectively.

## METHOD

In the method used here (Gephart and Forsyth, 1984) the minimum misfit is found by

**Table 1 - Main location parameters of the earthquakes investigated in this work.**
Order number, date, epicenter latitude and longitude, focal depth, total number of P and S readings used for the hypocentral computation, network azimuthal gap, arrival-time rms, epicenter and depth errors, and location quality (standard definitions from the HYPO71 program are used; see for example Lee and Valdes, 1989). The "area" is indicated only for the 35 events with good-quality location and FPS: Sis, Vul and Cal mean, respectively, Sisifo, Vulcano and Calabrian Arc; Dep and Out mean sub-crustal events of the Tyrrhenian Sea and events external to the previous sets (see Fig. 4). The hypocentral computations were done using the HYPO71PC computer program (Lee and Valdes, 1989) and a 1-D velocity model with station corrections recently determined for the region (Neri et al., 1991). The last variable (Pol) in this table represents the ratio between the number of polarities in agreement with the fault plane solution and the total number of polarities.

| N | Day | Hour | Lat | Lon | Dep | No | Gap | rms | ERH-Z | Q | Area | Pol |
|---|---|---|---|---|---|---|---|---|---|---|---|---|
| 1 | 880308 | 0840 | 38 23 | 15 52 | 33 | 29 | 111 | 0.56 | 2.8 1.7 | C | | |
| 2 | 880330 | 1119 | 38 25 | 14 46 | 15 | 20 | 164 | 0.51 | 2.7 3.3 | D | | |
| 3 | 880401 | 2343 | 37 42 | 15 12 | 03 | 23 | 135 | 0.53 | 1.6 2.5 | D | | |
| 4 | 880406 | 0125 | 38 34 | 14 45 | 08 | 33 | 137 | 0.60 | 2.4 1.5 | C | Sis | 11/14 |
| 5 | 880411 | 0150 | 38 07 | 15 07 | 12 | 22 | 74 | 0.47 | 1.3 1.4 | B | | |
| 6 | 880417 | 0231 | 37 47 | 15 01 | 20 | 22 | 114 | 0.49 | 1.6 2.1 | C | | |
| 7 | 880417 | 0605 | 38 24 | 14 42 | 14 | 22 | 172 | 0.54 | 3.0 1.6 | D | | |
| 8 | 880417 | 1520 | 38 22 | 14 47 | 12 | 18 | 166 | 0.52 | 3.0 1.5 | D | | |
| 9 | 880528 | 0557 | 38 19 | 14 49 | 20 | 24 | 103 | 0.47 | 1.6 2.3 | C | Sis | 11/12 |
| 10 | 880530 | 1006 | 38 26 | 14 42 | 12 | 28 | 106 | 0.68 | 2.5 1.8 | C | Sis | 10/10 |
| 11 | 880604 | 1628 | 38 24 | 14 42 | 09 | 29 | 98 | 0.66 | 1.9 1.7 | D | | |
| 12 | 880605 | 1243 | 38 25 | 14 40 | 12 | 33 | 104 | 0.69 | 1.9 1.5 | C | Sis | 15/16 |
| 13 | 880610 | 0131 | 38 11 | 15 11 | 11 | 27 | 58 | 0.54 | 1.3 1.7 | C | Vul | 14/15 |
| 14 | 880721 | 1718 | 37 57 | 15 42 | 33 | 25 | 138 | 0.43 | 2.1 2.1 | C | Cal | 12/12 |
| 15 | 880721 | 2229 | 37 45 | 14 42 | 13 | 39 | 89 | 0.72 | 1.6 2.1 | C | | |
| 16 | 880723 | 1758 | 38 43 | 15 38 | 85 | 42 | 78 | 0.39 | 1.5 2.7 | B | Dep | 25/26 |
| 17 | 881007 | 1622 | 38 30 | 14 38 | 11 | 36 | 125 | 0.51 | 1.8 1.2 | C | Sis | 9/10 |
| 18 | 881022 | 0035 | 38 35 | 16 07 | 10 | 28 | 100 | 0.42 | 1.2 1.3 | C | Cal | 11/12 |
| 19 | 881107 | 1426 | 38 08 | 15 50 | 15 | 36 | 101 | 0.76 | 2.0 2.6 | C | Cal | 14/18 |
| 20 | 881108 | 0702 | 38 05 | 15 50 | 13 | 22 | 133 | 0.63 | 2.3 1.4 | C | | |
| 21 | 881108 | 0813 | 38 06 | 15 50 | 22 | 23 | 122 | 0.48 | 2.2 1.8 | C | | |
| 22 | 881108 | 1504 | 38 24 | 15 45 | 09 | 25 | 81 | 0.46 | 1.3 1.6 | C | | |
| 23 | 881211 | 2356 | 37 52 | 15 00 | 13 | 23 | 107 | 0.70 | 2.8 2.5 | C | | |
| 24 | 890117 | 1652 | 38 37 | 15 37 | 93 | 17 | 119 | 0.39 | 3.8 11. | C | | |
| 25 | 890123 | 0822 | 37 51 | 15 32 | 18 | 18 | 148 | 0.40 | 1.7 2.8 | C | Cal | 10/12 |
| 26 | 890211 | 1207 | 38 36 | 15 29 | 55 | 33 | 97 | 0.41 | 1.6 3.1 | C | | |
| 27 | 890425 | 0108 | 37 59 | 14 06 | 10 | 28 | 66 | 0.75 | 2.2 1.6 | C | Out | 10/10 |
| 28 | 890502 | 1148 | 38 31 | 14 45 | 08 | 21 | 150 | 0.58 | 3.4 1.8 | C | Sis | 10/10 |
| 29 | 890526 | 2219 | 38 09 | 15 08 | 12 | 30 | 64 | 0.54 | 1.2 1.1 | C | Vul | 14/14 |
| 30 | 890619 | 2122 | 37 49 | 16 14 | 60 | 32 | 215 | 0.65 | 3.7 4.1 | D | | |
| 31 | 890621 | 1646 | 38 11 | 15 02 | 12 | 28 | 46 | 0.75 | 2.1 1.9 | C | Vul | 14/14 |
| 32 | 890622 | 1631 | 38 12 | 15 03 | 09 | 30 | 56 | 0.50 | 1.1 1.5 | C | | |
| 33 | 890624 | 0234 | 37 51 | 14 43 | 13 | 32 | 87 | 0.85 | 2.1 1.9 | C | Out | 11/17 |
| 34 | 890717 | 1357 | 37 35 | 16 12 | 13 | 22 | 227 | 1.27 | 9.3 15. | D | | |
| 35 | 890718 | 0508 | 38 29 | 14 46 | 11 | 46 | 101 | 0.73 | 1.8 1.1 | C | Vul | 14/15 |
| 36 | 890725 | 0147 | 38 32 | 15 34 | 89 | 15 | 86 | 0.57 | 5.7 12. | C | Dep | 12/12 |
| 37 | 890809 | 0324 | 39 08 | 15 14 | 239 | 34 | 107 | 0.49 | 4.1 7.6 | C | | |
| 38 | 890829 | 2246 | 38 18 | 15 40 | 09 | 27 | 89 | 0.46 | 1.2 1.2 | B | Cal | 10/10 |
| 39 | 890912 | 0132 | 38 25 | 14 42 | 12 | 31 | 89 | 0.48 | 1.5 1.1 | C | Sis | 11/11 |
| 40 | 890926 | 1638 | 38 31 | 14 37 | 14 | 31 | 93 | 0.62 | 2.6 1.4 | C | Sis | 12/15 |
| 41 | 891105 | 0226 | 38 27 | 14 57 | 08 | 28 | 86 | 0.60 | 1.8 1.2 | C | | |
| 42 | 900208 | 1750 | 38 58 | 16 15 | 09 | 27 | 91 | 0.49 | 1.5 1.6 | C | Cal | 9/10 |
| 43 | 900218 | 0028 | 38 07 | 15 08 | 23 | 43 | 76 | 0.49 | 1.0 1.5 | B | Vul | 19/21 |
| 44 | 900226 | 0311 | 38 38 | 14 23 | 20 | 30 | 117 | 0.64 | 2.6 2.3 | C | Sis | 10/12 |
| 45 | 900325 | 1823 | 39 08 | 15 17 | 32 | 23 | 142 | 1.37 | 6.9 32. | D | | |

**Table 1 (continued)**

| N | Day | Hour | Lat | Lon | Dep | No | Gap | rms | ERH-Z | Q | Area | Pol |
|---|---|---|---|---|---|---|---|---|---|---|---|---|
| 46 | 900328 | 0547 | 38 09 | 14 55 | 24 | 35 | 40 | 0.54 | 1.4 1.7 | C | Vul | 27/28 |
| 47 | 900404 | 1503 | 38 15 | 15 04 | 15 | 29 | 73 | 0.66 | 1.6 3.8 | C | Vul | 13/14 |
| 48 | 900418 | 1923 | 38 14 | 16 38 | 29 | 24 | 224 | 0.55 | 5.5 2.5 | D | | |
| 49 | 900510 | 0647 | 38 16 | 15 31 | 21 | 26 | 61 | 0.61 | 2.3 2.4 | C | Cal | 17/17 |
| 50 | 900601 | 2152 | 37 45 | 15 05 | 09 | 25 | 119 | 0.85 | 2.5 2.8 | D | | |
| 51 | 900915 | 0311 | 38 08 | 15 51 | 17 | 28 | 103 | 0.48 | 1.5 1.3 | C | Cal | 13/13 |
| 52 | 900922 | 1005 | 38 42 | 15 10 | 09 | 24 | 152 | 0.47 | 1.7 1.6 | C | | |
| 53 | 901005 | 2305 | 37 48 | 16 10 | 17 | 28 | 211 | 0.74 | 3.6 5.4 | D | | |
| 54 | 901111 | 0911 | 38 26 | 15 24 | 100 | 27 | 96 | 0.59 | 3.6 3.3 | C | Dep | 11/13 |
| 55 | 901218 | 0438 | 38 09 | 15 11 | 10 | 21 | 91 | 0.43 | 1.4 1.6 | C | Vul | 10/10 |
| 56 | 901218 | 1749 | 38 07 | 15 09 | 09 | 20 | 74 | 0.48 | 1.5 1.6 | C | | |
| 57 | 901223 | 1916 | 38 45 | 15 28 | 75 | 29 | 154 | 0.67 | 3.7 4.6 | D | | |
| 58 | 910210 | 1258 | 37 45 | 16 03 | 09 | 25 | 216 | 1.97 | 7.5 6.6 | D | | |
| 59 | 910427 | 0057 | 38 47 | 15 40 | 62 | 27 | 121 | 0.45 | 2.4 4.4 | C | Dep | 17/17 |
| 60 | 910518 | 1008 | 38 30 | 15 25 | 65 | 32 | 114 | 0.60 | 2.6 3.5 | C | | |
| 61 | 910606 | 0109 | 38 21 | 16 23 | 74 | 37 | 192 | 0.50 | 2.9 2.8 | D | | |
| 62 | 910804 | 0139 | 37 45 | 16 19 | 15 | 34 | 231 | 0.54 | 2.5 2.4 | D | | |
| 63 | 910821 | 0242 | 39 03 | 15 57 | 52 | 30 | 107 | 0.34 | 1.5 3.3 | C | Dep | 12/14 |
| 64 | 910906 | 1559 | 39 02 | 15 33 | 09 | 36 | 100 | 0.56 | 1.4 1.9 | D | | |
| 65 | 910907 | 0539 | 38 00 | 15 29 | 10 | 40 | 105 | 0.57 | 1.2 1.3 | C | | |
| 66 | 910924 | 0004 | 37 41 | 14 53 | 28 | 28 | 131 | 0.59 | 2.0 1.7 | C | Out | 12/12 |
| 67 | 910925 | 1321 | 38 02 | 16 00 | 16 | 22 | 176 | 0.50 | 2.3 1.9 | C | Cal | 13/15 |
| 68 | 910925 | 1453 | 38 01 | 16 01 | 17 | 28 | 148 | 0.53 | 2.0 1.6 | C | Cal | 14/16 |
| 69 | 910925 | 2121 | 38 00 | 16 01 | 15 | 32 | 197 | 0.77 | 2.7 1.4 | D | | |
| 70 | 910930 | 0549 | 37 37 | 16 27 | 28 | 23 | 247 | 0.75 | 4.7 3.1 | D | | |
| 71 | 911003 | 0240 | 38 51 | 15 12 | 12 | 36 | 107 | 0.58 | 1.6 1.4 | C | | |
| 72 | 911011 | 0014 | 37 37 | 16 25 | 19 | 31 | 241 | 1.10 | 4.4 3.7 | D | | |
| 73 | 911215 | 0552 | 39 10 | 16 05 | 21 | 16 | 159 | 0.41 | 2.3 2.3 | D | | |

a grid search in which the assumed orientation of the stress tensor is varied. For each orientation of the stress tensor, the misfits of the slip vector in both nodal planes for all of the individual focal mechanisms are computed, and from these the average misfit of the better fitting planes is evaluated. The misfit of an individual fault-plane solution is defined as the minimum rotation angle, about any axis, that brings into agreement the orientation of one of the observed fault-planes with the computed fault-plane and its slip vector (Gephart and Forsyth, 1984). In addition to the stress tensor orientation with the minimum misfit, the grid search yields all solutions for which the misfit cannot be distinguished from the smallest misfit at an assigned confidence level (Parker and Mc Nutt, 1980; Gephart and Forsyth, 1984). The data input consists of the individual fault-plane solutions from a sub-volume of the study area. A weight is given to each earthquake based on the solution quality. The method gives the option to choose the plane of faulting over the auxiliary plane, if independent geological data allow such a choice. If a choice is not made as part of the input (as in the present work) the plane with the smaller misfit is chosen as the fault-plane during the inversion process.

The main steps in our application of the algorithm for inverting fault plane solutions for stress tensor directions can be summarized as follows:

(1) A stress configuration is assumed by giving specific values to the directions of the principal stresses and to the R parameter given by [sigma1-sigma2] / [sigma1-sigma3] (where sigma1, sigma2 and sigma3 are the principal stress magnitudes).

(2) From a family of hypothetical fault-planes, with slip vectors in the directions of the shear stress resolved in each plane, the two are selected which require the smallest rotation about any axis to bring plane and slip vector into the position observed for the two nodal planes of each earthquake.

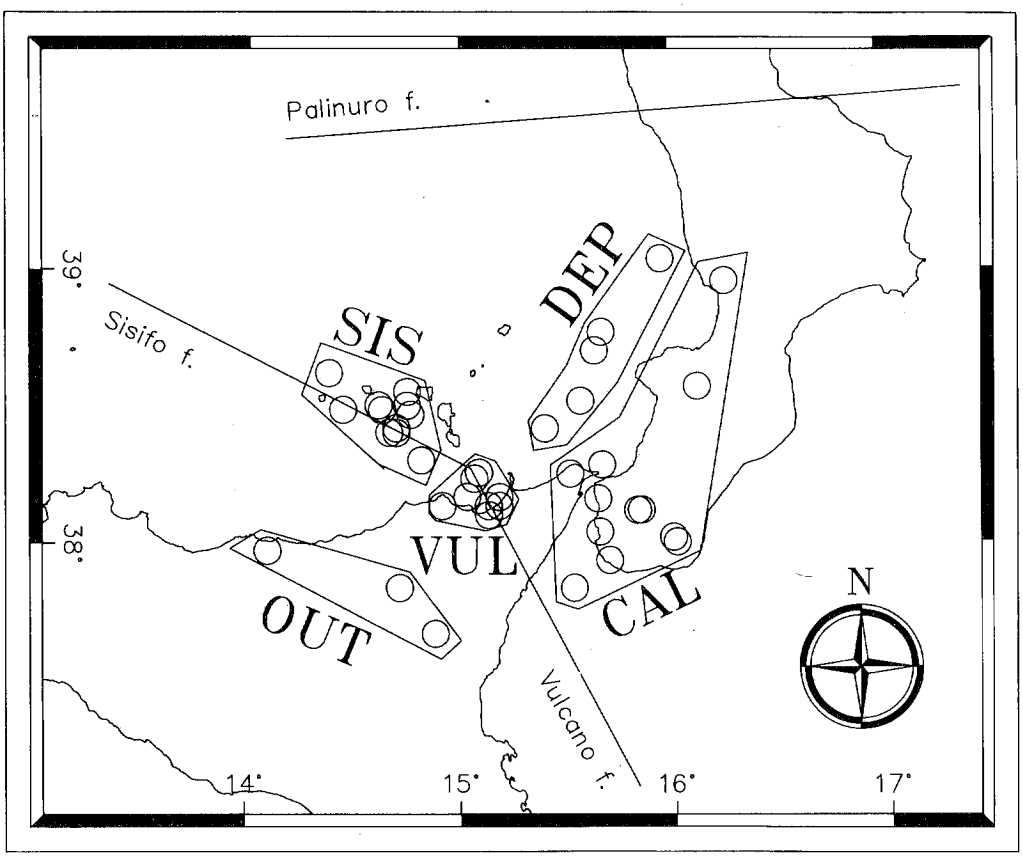


Fig. 4 - Epicenter distribution for the earthquake sample, which includes 35 good quality events analyzed in this work (period 1988-1991, Table 1) and four additional events taken from the literature (1908 Messina earthquake, Schick, 1979; 1978 and 1980 Aeolian Islands earthquakes, Gasparini et al., 1982; 1985 Messina earthquake, Bottari et al., 1989). The polygons define the volumes used for generating the sets submitted to stress tensor inversion (see text).

(3) The smaller of the two rotations is selected as the misfit angle for each earthquake, assuming that the nodal plane with the closer agreement with the assumed stress directions was the fault-plane.

(4) The average misfit based on all earthquakes in the data set is computed.

(5) Steps 1 through 4 are repeated for numerous positions of the assumed stress tensor, covering a range of selected positions with a grid. The range may include all possible directions.

(6) Steps 1 through 5 are repeated for a range of R-values.

(7) The stress directions and the R-value leading to the minimum average misfit are selected as the best fit and used as the solution.

(8) The stress directions and R-values that cannot be distinguished from the best solution at a given confidence level are identified according to the method described by Gephart and Forsyth (1984) and Parker and McNutt (1980).

(9) The quality of the solution is assessed by examining the size of the average misfit, and the circumstances of those earthquakes that show misfits larger than the uncertainties in the fault plane solutions. For a preliminary discussion of the relationship between the misfit defined by Gephart and Forsyth (1984) and the quality of a solution, see Wyss et al. (1992).

(10) If a pattern of misfit size as a function of location or time emerges, the limits of the data set may be redefined and steps 1 through 9 repeated.

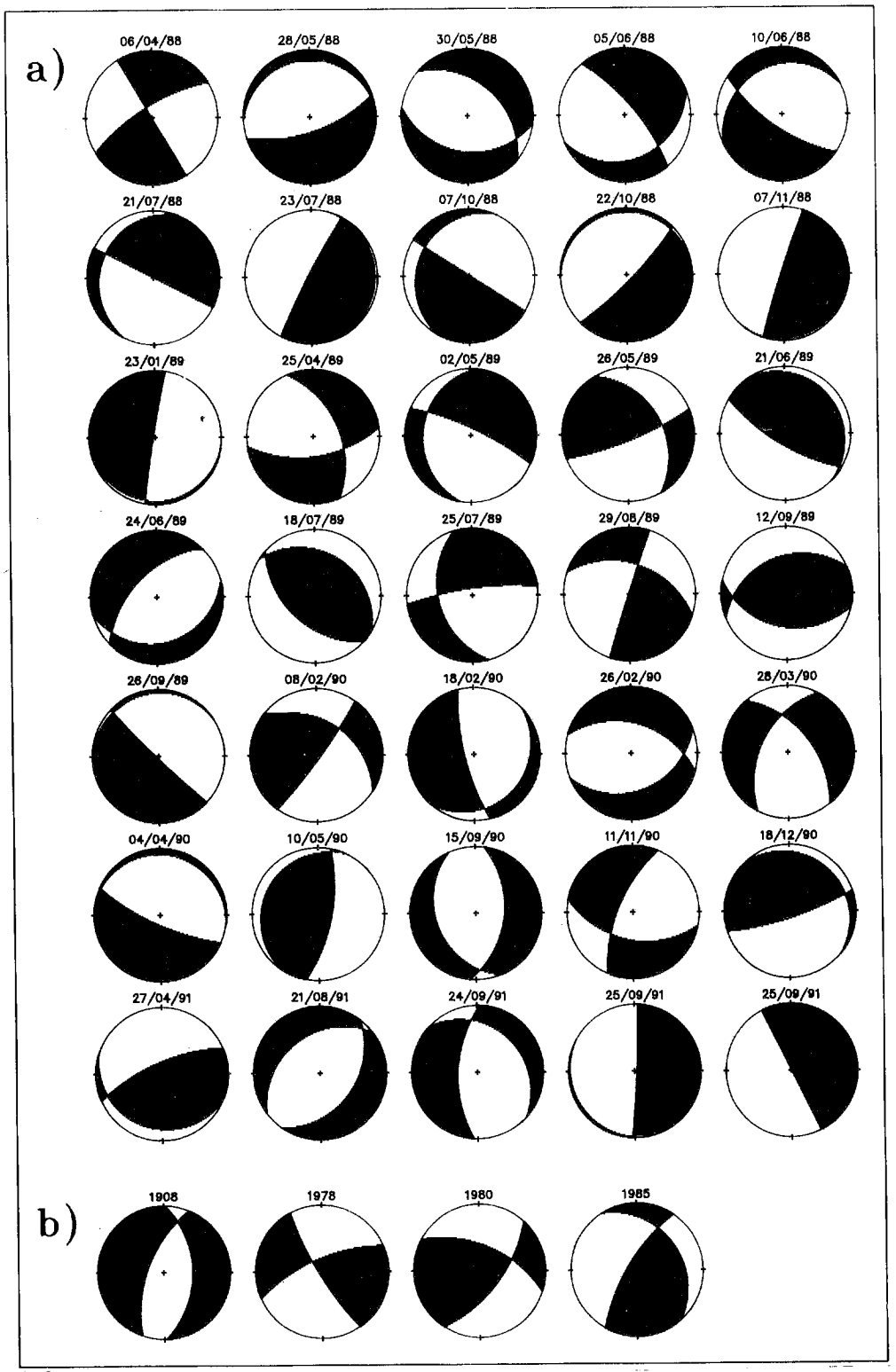


Fig. 5 - Fault plane solutions of the earthquakes reported in Fig. 4:
a) events analyzed in the present work (1988-1991; Table 1);
b) data from literature (see caption of Fig. 4 for details).

This method will find all the minima for the average misfit as a function of stress orientation if appropriate grids are used; for this reason it is generally more efficient with respect to the other stress inversion algorithms which are based on the maximization of likelihood functions. For large data sets, computing time may become a problem requiring powerful computers, but for the small data sets used here, the CPU times on PCs were reasonable.

In a crustal volume which contains only one major fault, or a system of parallel faults, with low frictional strength, all earthquakes would occur along these faults with slip vectors parallel to the shear stress resolved in the plane, regardless of the angle maintained between this plane of weakness and the principal stress. In this case, all the fault plane solutions would be the same, and the directions of the principal stresses would be as poorly constrained as in the case of a single fault-plane solution (Mc Kenzie, 1969). If, however, a crustal volume contains planes of weakness with varying orientations, then very different types of fault-plane solutions will result, even from a single homogeneous stress tensor orientation. In this case, the inversion method may be able to constrain the directions of the stress tensor accurately, because only a narrow range of orientations can produce the observed slip on the fault-planes with varying orientations. Thus the inversion results are firstly judged by the quality of fit. However, the stress orientation constraint is judged by the confidence limits of the result. In the first example above (fault-plane solutions with similar orientations), the quality of fit would be excellent (misfit close to 0), but the usefulness would be poor because the confidence limits would be very large; that is, many stress directions would be almost equally admissible. In the second example, the confidence limits would cover only a small area of the stereo net around the preferred solution, and hence this state of stress could be distinguished relatively easily from another one in a different crustal volume or at a different time.

In each attempt to invert for the stress tensor direction by the above cited technique, one makes the assumption that the stress tensor is spatially and temporally homogeneous. As Michael (1987a) has shown, the choice of the smaller misfit in each fault-plane solution may lead to a bias for finding a homogeneous stress tensor with a reasonably small misfit, even for cases where data sets from volumes with significantly different stress tensor orientations have been mixed. Therefore, one cannot be completely sure, based on a inversion result, that one is dealing with a homogeneous distribution of the stress tensor throughout the volume under consideration. Nevertheless, the size of the average misfit provides a guide to how well the assumption of homogeneity is fulfilled (Michael, 1987a). It is possible to define differences between sub-volumes, if one can show that separate inversions lead to stress tensor orientations for which the confidence limits do not overlap, and for which the individual misfits are smaller than for the inversion considering the entire volume. Conversely, if the inversion leads to the same result in several sub-volumes, it is reasonable to propose that the stress tensor orientation is homogeneous throughout these volumes. In the light of the results of a series of tests carried out by Wyss et al. (1992b) for identifying the relationship between FPS uncertainties and minimum average misfit in the case of uniform stress distribution, we will assume in this work that the condition of a homogeneous stress tensor is fulfilled if the misfit is smaller than 10 degrees. For solutions with larger misfits we suspect that the assumption of homogeneity is not fulfilled.

## RESULTS AND DISCUSSION

The events "Dep" in Table 1 and Fig. 4 are located in the depth range 50-100 km, so that they are clearly deeper than all others (Sis, Vul, Cal, Out) which lie within the crust. Because the assumption of stress uniformity in a 100 km thick volume is quite unreasonable, and the number of such sub-crustal events is too low for defining a sub-volume including only them and making a separate inversion, the "Dep" events were eliminated from the sample. The remaining earthquakes were utilized for generating five sets: SISIFO (Sis, Tab. 1 and Fig. 4), VULCANO (Vul), CALABRIANARC (Cal), AEOLIAN (Sis and Vul), REGION (Sis, Vul, Cal and Out). It can be deduced from Fig. 5 that each of these sets is characterized by some heterogeneity of the fault-plane solutions, and this is one of the basic conditions to be fulfilled in order to avoid indeterminacy in the stress computations (see the section "Method"). Each

**Table 2 - Best stress models obtained for all volumes investigated in this work.**
M.A.M. means "minimum average misfit" (see the section "Method"). The stress models obtained for the Sisifo, Vulcano and Calabrianarc sub-volumes are also graphically represented in Fig. 6.

| VOL | SIGMA 1 | | SIGMA 2 | | SIGMA 3 | | R | M.A.M. |
|---|---|---|---|---|---|---|---|---|
| | dip | azim | dip | azim | dip | azim | | |
| REG | 77 | 195 | 12 | 355 | 4 | 86 | 0.1 | 19.1 |
| AEO | 63 | 158 | 1 | 66 | 27 | 334 | 0.1 | 16.4 |
| SIS | 36 | 288 | 29 | 42 | 40 | 160 | 0.1 | 8.4 |
| VUL | 2 | 24 | 36 | 115 | 54 | 291 | 0.3 | 4.5 |
| CAL | 87 | 80 | 2 | 301 | 2 | 211 | 0.3 | 7.9 |

set was submitted to stress tensor inversion. For each set, several tests were performed by using different grid steps and a large variety of starting values for the stress parameters, in order to check the reliability of the results. The best models are reported in Table 2.

First, it can be observed that sets REGION and AEOLIAN are characterized by fairly high values of the minimum average misfit (see section "Method"), which basically corresponds to a relatively high number of earthquakes in each set showing a minimum misfit higher than the FPS uncertainties. Second, the stress directions estimated for the SISIFO, VULCANO and CALABRIANARC sub-regions (see next paragraph) differ from each other. These observations indicate that the assumption of stress space-time uniformity in the whole region considered (set REGION) and in the Aeolian Islands area only (AEOLIAN) is not acceptable. Additional computations not reported here show that this holds also if the events of 1908, 1978, 1980 and 1985 (Fig. 5b) are excluded from the two sets and, then, the time extension of the respective samples is reduced to a few years (1988-1991). Thus, we conclude that the stress directions are not uniform throughout the study area. This result agrees with the available information on the tectonic processes in the region and with the high degree of structural heterogeneity (section "Geodynamic context"). It has already been emphasized that, in spite of the relatively small extent of the area investigated, it is characterized by quite heterogeneous geodynamic situations; these are represented, for example, by the presence both of tensional and compressive forces in the model for the processes in the Messina Straits at different depth levels (Fig. 3), and by the fault trend variation from NW-SE to N-S approximately, in the framework of the strike- slip dislocation processes at the southern margin of the Tyrrhenian area (Aeolian Islands, Sisifo and Vulcano faults, Figs. 1 and 2). In particular, the last aspect is explainable in terms of space differentiation of the crust generation process, with sources located along the Selli line and in the Marsili basin, respectively; such a differentiation may be one reason for the bad fit obtained for the set AEOLIAN.

For the other three sets (SISIFO, VULCANO and CALABRIANARC) values for the minimum average misfit in the range 4°-9° have been found. This suggests that the assumption of uniform stress within each sub-region may be fulfilled. Although this cannot be further tested by subdividing into smaller data sets, we believe it is reasonable to assume that the stress directions are homogeneous because the misfits are small. It is interesting to observe that in all of these cases the direction of the principal stress is in agreement with the available geodynamic information (Fig. 6). The sigma1 azimuth for the SISIFO set is compatible with a stress source located along the Selli rifting line. The sigma1 dip may be related to the presence of asperities at the crust-mantle transition along this fault system (Neri et al., 1991). For the VULCANO set, the principal stress (which is nearly horizontal in this case) may derive from the crustal generation process in the Marsili basin. Finally, in the Calabrian arc, the seismically dominant presence of the tensional structures finds some evidence in the vertical sigma1 direction obtained for the corresponding earthquake set.

However, as has been repeatedly said above, a limitation of the present approach to stress inversion is represented by the low number of earthquakes available in relation to sub-volumes SISIFO, VULCANO and CALABRIANARC (9, 10 and 12, respectively). A quite obvious doubt arises as to what extent the stress solutions are constrained. The confidence limits have been evaluated following the statistical procedure described in Parker and McNutt (1980) and in

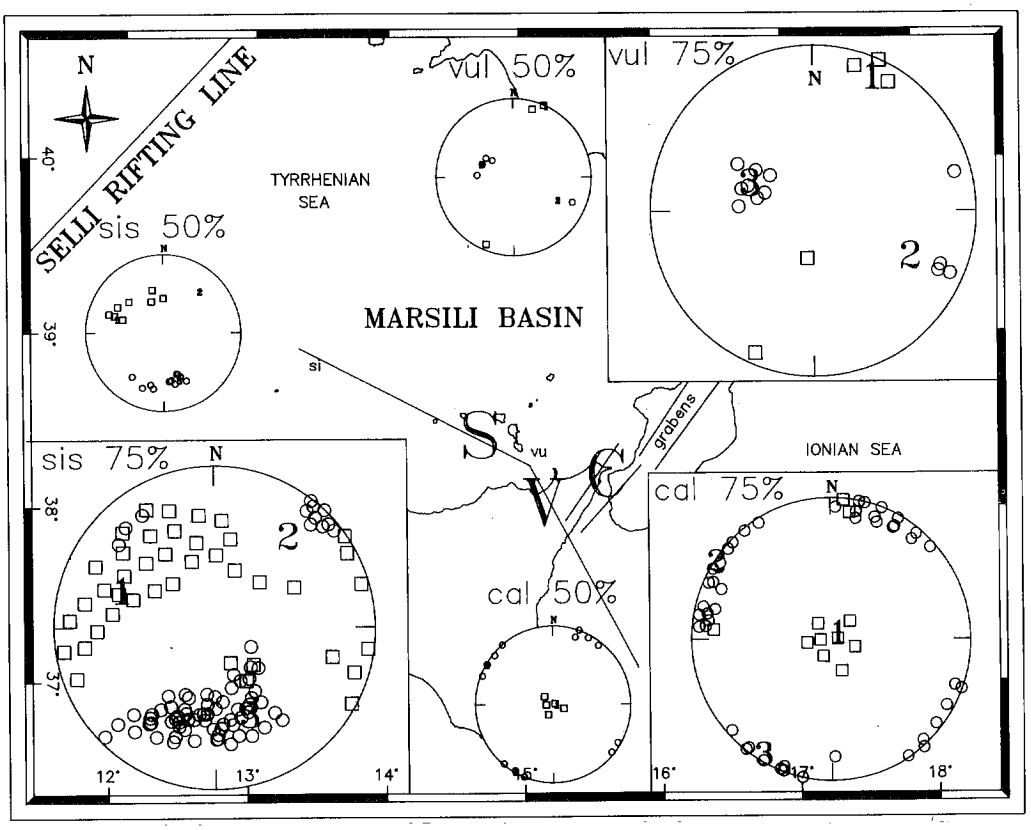


Fig. 6 - Stereographic projections of the stress tensor inversion results obtained for the SISIFO, VULCANO and CALABRIANARC sub-volumes (S, V and C in the map). Confidence limits are evaluated at the 75% and 50% levels. The numbers 1, 2 and 3 indicate the directions of the best fitting greatest, intermediate and least principal stresses, respectively. Squares and circles mark positions of the greatest and least principal stresses for which the solution cannot be distinguished from the best fit. Also, some tectonic features of the region (already described in the "Geodynamic context" section) are schematically reported in order to allow an immediate comparison with the stress tensors.

Gephart and Forsyth (1984) and adopting, as in those works, different values for the probability threshold (50%, 75%, 90%, and 95%, respectively). We found that the best solutions for the stress directions in the three sub-regions are quite different, but they cannot be differentiated at the 95% and 90% confidence levels, because the areas of equivalent solutions on the stereographic projections overlap. However, at the 75% confidence level these areas are close to not overlapping (Fig. 6), so that we can distinguish the different stress tensors in the three sub-regions at a confidence level between 50% and 75%. Although it will be necessary to increase the confidence level to 90% or 95% in the future, we propose that the preliminary estimates for the stress directions in SIS, VUL and CAL (Table 2, Fig. 6) are close to correct, and differ from each other by as much as 90°. With regard to the data limitations, the following aspects should be stressed. Firstly, the available sample is not adequate in relation to the degree of complexity of the local geodynamic situation which, as said above, is high. Secondly, during the earthquake selection done to prepare the input data for the stress tensor inversion, many events were excluded because of the low quality of hypocenter locations and fault-plane solutions. Although data from several tens of stations were available for these events, the network geometry was poor. This is easily understandable from the station map of Fig. 1. Thus it is evident that the installation of ocean bottom seismometers in the Tyrrhenian and Ionian seas would greatly help to extend this investigation; in addition, it would help to define a 3-D earth velocity model for the region, which is also important for increasing the quality of the input data to the stress tensor inversion.

## CONCLUSIONS

The first conclusion of this work is that the bad fit obtained for the whole set of crustal events (REGION), together with the improvement of the fit in sub-regions, indicates that the stress field is not uniform in the area investigated. The same conclusion may be drawn with regard to the Aeolian Islands sub-volume, which includes two of the main fault systems in the region (the Sisifo and Vulcano ones). These results are in agreement with the available information on the tectonic processes in the region, and with the high degree of structural heterogeneity.

However, separate inversions for the two groups of events located near the Sisifo and Vulcano fault systems, respectively, lead to quite low values of all minimum misfits. The two best models match well with the local geology and tectonics. In particular, the sigma1 direction for the SISIFO set is compatible with a stress source located along the Selli rifting line (Fig. 6). For the VULCANO set, the principal stress may derive from the crust generation process in the Marsili basin (Fig. 6). A low value of the minimum average misfit is also obtained in the Calabrian arc area, where the inversion method determines, as best model, the stress field closest to the known geodynamical features of the area (graben dynamics, Fig. 6).

The main problem is the quite low constraint of the models, due to the small number of earthquakes available for each of sub-volumes SISIFO, VULCANO and CALABRIANARC. Quantitatively speaking, the stress fields in the three sub-volumes differ at a confidence level between 50% and 75%.

In conclusion, the results of this work evidence some stress heterogeneity in the region investigated and seem to support, though at a very preliminary level, the available information on the local tectonics. More data are needed for putting adequate constraints on the stress model of each of the sub-volumes investigated. The results presented here strongly demonstrate the need for further effort in development of the network, and clearly display immediate implications.

## REFERENCES


Anderson H. and Jackson J.; 1987: *The deep seismicity of the Tyrrhenian Sea.* Geophys. J.R. Astr. Soc., **91**, 613-637.

Barberi F., Gasparini P., Innocenti F. and Villari L.; 1973: *Volcanism of the Southern Tyrrhenian Sea and its geodynamic implications.* J. Geophys. Res., **78**, 23, 5221-5232.

Bottari A. and Lo Giudice E.; 1987: *Structural studies on the Strait of Messina.* The seismotectonic data. Doc. et Trav. IGAL n011, 115-125.

Bottari A., Capuano P., De Natale G., Gasparini P., Neri G., Pingue F. and Scarpa R.; 1989: *Source parameters of earthquakes in the Strait of Messina, Italy, during this century.* Tectonophysics, **166**, 221-234.

Burton A.N.; 1964: *Marine levels in South Italy.* Nature, **203**, 1060.

Calcagnile G. and Panza G.F.; 1981: *The main characteristics of the lithosphere-astenosphere system in Italy and surrounding regions.* PAGEOPH, **119**, 865-879.

Calcagnile G., D'Ingeo F., Farrugia P. and Panza G.F.; 1982: *The lithosphere in the Central-Eastern Mediterranean area.* PAGEOPH, **120**, 389-406.

Colombi B., Giese P., Luongo G., Morelli C., Riuscetti M., Scarascia S., Schutte K.G., Strowald J. and De Visentini G.; 1973: *Preliminary report on the seismic refraction profile Gargano-Salerno-Palermo-Pantelleria (1971).* Boll. Geof. Teor. Appl., **15**, 225-254.

Falsaperla S., Frazzetta G., Neri G., Nunnari G., Velardita R. and Villari L.; 1989: *Volcano monitoring in the Aeolian Islands (Southern Tyrrhenian Sea): The Lipari-Vulcano euptive complex.* IAVCEI proceedings in Volcanology, 1, J.H. Latter Editor, Volcanic Hazard, 339-356.

Finetti I. and Del Ben A.; 1986: *Geophysical study of the Tyrrhenian opening.* Boll. Geof. Teor. Appl., **28**, 75-155.

Frazzetta G., Lanzafame G. and Villari L.; 1982: *Deformazioni e tettonica attiva a Lipari e Vulcano (Eolie).* Mem. Soc. Geol. It., **24**, 293-297.

Gasparini C., Iannaccone G., Scandone P. and Scarpa R.; 1982: *Seismotectonics of the Calabrian Arc.* Tectonophysics, **84**, 267-286.

Gephart J.W. and Forsyth D.W.; 1984: *An improved method for determining the regional stress tensor using earthquake focal mechanism data: application to the San Fernando earthquake sequence.* J. Geophys. Res., **89**, 9305-9320.

Ghisetti F.; 1980: *Caratterizzazione dei blocchi della Calabria Meridionale in base alla velocità di sollevamento nel Plio-Pleistocene: una proposta di zonazione neotettonica.* CNR, P.F. Geodinamica, Pubbl. n° 356.

Ghisetti F. and Vezzani L.; 1982: *Different styles of deformation in the Calabrian Arc (Southern Italy): implications for a seismotectonic zoning.* Tectonophysics, **85**, 149-165.

Ghisetti F.; 1984: *Recent deformations and the seismogenic source in the Messina Strait (Southern Italy).* Tectonophysics, **109**, 191-208.

Gillard D., Wyss M. and Nakata J.S.; 1992: *A seismotectonic model for Western Hawaii based on stress tensor inversion from fault plane solutions.* J. Geophys. Res., **97**, 6629-6641.

Hauksson E.; 1990: *Earthquake faulting and stress in the Los Angeles basin.* J. Geophys. Res., **95**, 15365-15394.

Jones L.M.; 1988: *Focal mechanisms and the state of stress on the San Andreas fault in Southern California.* J. Geophys. Res., **93**, 8869-8891.

Lee W.H.K. and Valdes C.M.; 1989: *User manual for HYPO71PC.* IASPEI Software Library, Toolbox for Seismic Data Acquisition Processing and Analysis, 1, 203-236.

Liang B. and Wyss M.; 1991: *Estimates of orientations of stress and strain tensors based on fault-plane solutions in the epicentral area of the great Hawaiian earthquake of 1968.* Bull. Seism. Soc. Am., **81**, 2320-2334.

Locardi E.; 1988: *The origin of the Appeninic arcs.* Tectonophysics, **146**, 105-123.

Loddo M. and Mongelli F.; 1979: *Heat flow in Italy.* PAGEOPH, **117**, 135-149.

Mantovani E., Babbucci D. and Farsi F.; 1985: *Tertiary evolution of the Mediterranean region: major outstanding problems.* Boll. Geof. Teor. Appl., **27**, 67-90.

Mantovani E., Babbucci D., Mucciarelli M. and Albarello D.; 1987: *Africa Eurasia kinematics.* In: Baldi P. and Zerbini S. (eds), Proceedings of the Third International Conference on the Wegener / Medlas Project. Esculapio, Bologna, 37-50.

Mantovani E., Babbucci D., Albarello D. and Mucciarelli M.; 1990: *Deformation pattern in the Central Mediterranean and behaviour of the African/Adriatic promontory.* Tectonophysics, **179**, 63-79.

Martini M. and Scarpa R.; 1983: *Earthquakes in Italy in the last century.* In: Proc. E. Fermi School of Physics, course LXXXV, Springer-Verlag, pp. 479-492.

McKenzie D.P.; 1969: *The relation between fault-plane solutions for earthquakes and the direction of the principal stresses.* Bull. Seism. Soc. Am., **59**, 591-601.

Michael A.J.; 1987a: *Use of focal mechanisms to determine stress: A control study:* J. Geophys. Res., **92**, 357-368.

Michael A.J.; 1987b: *Stress rotation during the Coalinga aftershock sequence.* J. Geophys. Res., **92**, 7963-7979.

Morelli C., Giese P., Cassinis R., Colombi B., Guerra I., Luongo G., Scarascia S. and Schutte K.G.; 1975: *Crustal structure of Southern Italy. A seismic refraction profile between Puglia- Calabria-Sicily.* Boll. Geof. Teor. Appl., **17**, 182-210.

Mulargia F. and Boschi E.; 1983: *The 1908 Messina earthquake and related seismicity.* In: Proc. E. Fermi School of Physics, course LXXXV, Springer-Verlag, pp. 493-518.

Mulargia F., Baldi P., Achilli V. and Broccio F.; 1984: *Recent crustal deformation and tectonics of the Messina Strait area.* Geophys. J. R. Astr. Soc., **76**, 369-381.

Neri G., Caccamo D., Cocina O. and Montalto A.; 1991: *Shallow earthquake features in the Southern Tyrrhenian region: geostructural and tectonic implications.* Boll. Geof. Teor. Appl., **33**, 129, 47-60.

Neri C., Caccamo D., Cocina O. and Montalto A.; 1993: *Geodynamic implications of recent earthquake data in Southern Tyrrhenian Sea.* Tectonophysics, submitted.

Oppenheimer D.H., Reasenberg P.A. and Simpson R.W.; 1988: *Fault plane solutions for the 1984 Morgan Hill, California, earthquake sequence: Evidence for the state of stress on the Calaveras fault.* J. Geophys. Res., **93**, 9007-9026.

Parker R.L. and Mc Nutt M.K.; 1980: *Statistics for the one norm misfit measure.* J. Geophys. Res., **85**, 4429-4430.

Patacca E. and Scandone P.; 1989: Post-Tortonian mountain building in the Appenines. The role of the passive sinking of a relic lithospheric slab. In: Atti Convegni Lincei, Acc. Naz. Lincei, Rome, **80**, pp. 157-176.

Patacca E., Sartori R. and Scandone P.; 1990: *Tyrrhenian basin and Appeninic arcs: kinematic relations since late tortonian times.* In: 75° Congress of the Soc. Geol. It., Milano, September 1990. In press on Mem. Soc. Geol. Ital..

Scandone P.; 1979: *Origin of the Tyrrhenian Sea and Calabrian Arc.* Boll. Soc. Geol. It., **98**, 27-34.

Scandone P. and Patacca E.; 1984: *Tectonic evolution of the Central Mediterranean area.* Ann. Geophys., **2**, 139-142.

Scarpa R.; 1982: *Travel-time residuals and three-dimensional velocity structure of Italy.* PAGEOPH, **120**, 583-606.

Schick R.; 1979: *A seismotectonic study of the 1908 Messina earthquake.* Tectonophysics, **53**, 289-290.

Whitcomb J.H., Allen C.R., Garmany J.D. and Hileman; 1973: *San Fernando earthquake series, 1971, focal mechanisms and tectonics.* Rev. Geophys., **11**, 693-730.

Wyss M., Gillard D. and Liang B.; 1992a: *An estimate of the absolute stress tensor in Kaoiki, Hawaii.* J. Geophys. Res., **97**, 4763-4768.

Wyss M., Liang B., Tanigawa W.R. and Wu X.; 1992b: *Comparison of orientations of stress and strain tensors based on fault plane solutions in Kaoiki, Hawaii.* J. Geophys. Res., **97**, 4769-4790.